4

RESULTS AND DISCUSSION

Under normal conditions fuel is kept stored in oil tanks for not more than a month or so. But for reserves of petroleum products keeping fuel stocks for a long term (as long as 8 years) is mandatory. However during that period microorganisms can appear in the stored fuel, remain at the bottom of the tank together with sediments and water. Since biofuels are more hygroscopic they absorb water from the atmosphere and the microbial growth is concentrated at the fuel/ water interface i.e emulsified water. Moreover the mono and diglycerides left over during transesterification process act as emulsifiers facilitating the growth of microorganisms.

4.1 Bacterial Isolation

In our laboratory where a two year old JBD left over from a previous research work was stored, a sediment formation was observed at the bottom of the stored vessel. The sediment was collected in a sterile container and serially diluted in a logarithmic manner and inoculated in the agar medium by pour plate technique and incubated for 24-48 h. Three bacterial strains isolated have been used for the present study. Preliminary identification of three bacterial strains obtained (having countable colonies ranging from 30-300) indicated that the isolates belonged to the genus *Bacillus sp*. **Figure 4a** gives the developed bacterial colonies in the petriplate and **Figure 4b** is the microscopic image of the isolated *Bacillus pumilus*.

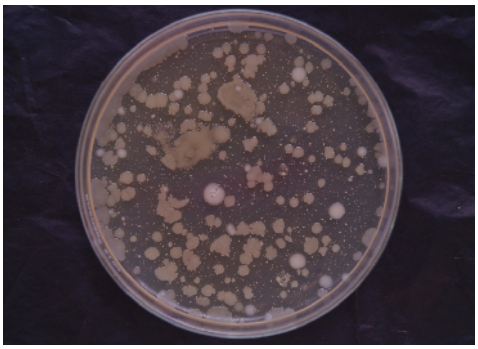

Figure 4a. Petriplate with bacterial colonies

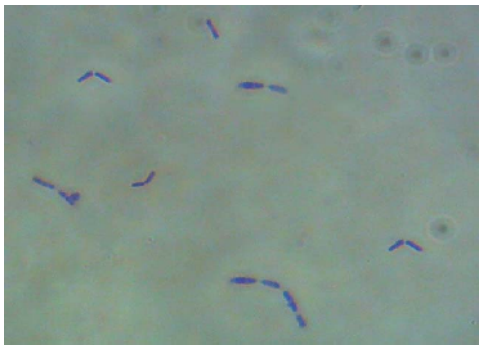

Figure 4b. Microscopic image of *Bacillus pumilus*

4.2. Identification of Bacteria

4.2.1 DNA extraction, PCR amplification and 16S rRNA gene sequence analysis.

DNA extraction was done and amplification of targeting bacterial16S rRNA gene was performed using eubacterial 16S rRNA primers

The 16S rRNA genes were cloned and the isolated plasmids from the clones were subjected to 16S rRNA gene sequencing. The sequences obtained were matched with the previously published sequences available in NCBI (National Centre for Biological Information) using BLAST.

Multiple sequence analysis was carried out with 16S rRNA sequences obtained from GenBank using CLUSTALX. Sequence alignment and comparison revealed similarity with ***Bacillus pumilus***. The nucleotide sequence data have been deposited in GenBank under the accession numbers **KF410588**, **KF410589** and **KF410590**.

4.3 Characterisation of Jatropha biodiesel

Biodiesel quality depends on several factors that reflect its chemical and physical characteristics. The quality of biodiesel can be influenced by a number of factors: the quality of the feedstock; the fatty acid composition of the parent vegetable oil or animal fat; the production process and other materials used in this process; the post-production parameters and the handling and storage. Given the fact that most current diesel engines are designed to be powered by diesel fuel, the physicochemical properties of biodiesel should be similar to those of diesel oil. Hence the JBD used in the present study was analysed for fuel properties in a testing laboratory. **Table 1** illustrates the comparison of the fuel properties of JBD against the standards ASTM D975 for pertrodiesel and ASTM D6751 for biodiesel.

Table 1. ASTM standards for diesel and biodiesel and fuel properties of *JBD*

Property	ASTM D975	ASTM D6751	Units	JBD
Flash Point	52.0 min	130.0 min	˚C	196
Water and Sediment	0.050 max	0.050 max	% vol	0.05
Kinematic Viscosity 40˚C	1.9 - 4.1	1.9 – 6.0	Mm2/sec	5.4
Sulphated Ash	0.01 max	0.020 max	% mass	0.02
Sulphur(S 500 grade)	0.05 max	0.05	% mass	0.0006
Copper strip corrosion	No 3 max	No 3 max		1
Cetane	40 min	47 max		53
Carbon residue		0.050 max	% mass	0.058
Acid number		0.80 max	Mg KOH/gm	2.72
Free Glycerin		0.020 max	% mass	0.02
Total Glycerin		0.240 max	% mass	0.25
Phospherous Content		0.001 max	% mass	0.0001
Distillation Temperature, Atmospheric Equivalent, 90% recovered	282 – 338	360 max	˚C	330
Aromaticity	35 max	-	% vol	

4.4. Corrosivity of *Jatropha curcas* biodiesel on the selected metals in the control and experimental systems

4.4.1 Mass loss measurements-Control system

While comparing the average corrosion rate of all the metals in JBD, its blends B5, B10, B20 and CD, though all the metals show highest corrosion rate in B100, a regular trend in the behaviour of the metals in the biodiesel mixtures could not be observed. Hence the most repeated trend in the corrosion rate of the studied metals has been taken to obtain the corrosion order of the metals. The order is found to be

Mild steel II ≈ Mild steel I > Brass > Copper > Aluminium

In other words the ferrous metals are found to be easily corroded by JBD than the nonferrous metals and alloys.

4.4.2 Mass loss measurements-Experimental system

Comparing the average corrosion rates of all the metals in JBD, its blends B5, B10 and B20 and CD in the presence of microorganism it is clear that all the metals except mild steel II show the highest corrosion rates in B100.Since as in the control system a regular trend in the behaviour of the metals in the test matrices could not be observed, the most repeated trend in the corrosion rate of studied metals has been taken to obtain the corrosion order of the metal. The order is found to be

Mild steel II > Mild steel I > Copper > Aluminium > Brass

Similar to the control system the propensity for corrosion of ferrous metals is higher than the non ferrous metals in the presence of bacteria.

4.4.3. Electrochemical Studies

MIC is an electrochemical process and hence electrochemical methods are used for studying biofilm/metal interface. (**Sooknah *et al*.2007).** The most frequently used electrochemical methods to monitor MIC are potentiodynamic polarisation technique and electrochemical impedance spectroscopy (EIS). Hence in the present work both these methods have been applied.

Potentiodynamic polarisation and electrochemical impedance data could not be taken, as the conductivity of the electrolyte in the presence of aluminium was too low to be measured indicating the low corrosion rate of aluminium. This in fact is in concurrence with the results of mass loss studies where the corrosion rate of the metal was the least both in the presence and absence of bacteria in various test matrices for 100 h.

4.5. Surface analysis

4.5.1. Optical microscopy

To support the results of mass loss studies the optical micrographs of the five metals aluminium, brass, copper, mild steel I and mild steel II in JBD and its blends with CD in the control and experimental systems were taken.

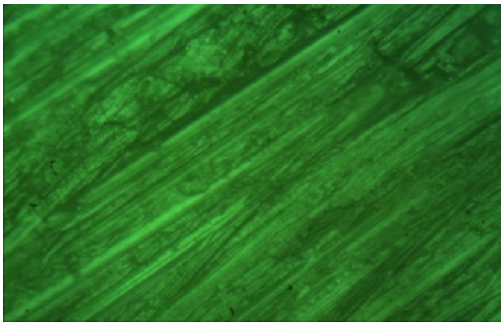

Aluminium

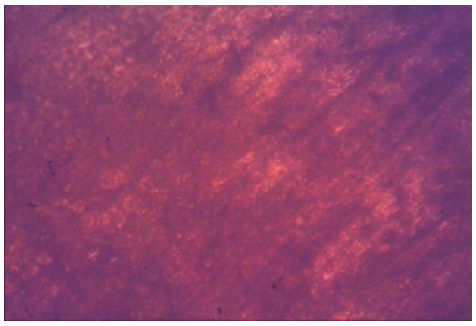

Brass

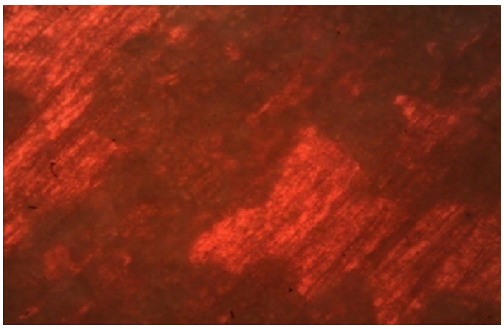

Copper

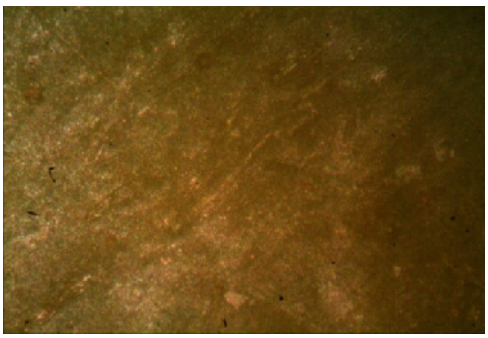

Mild Steel I

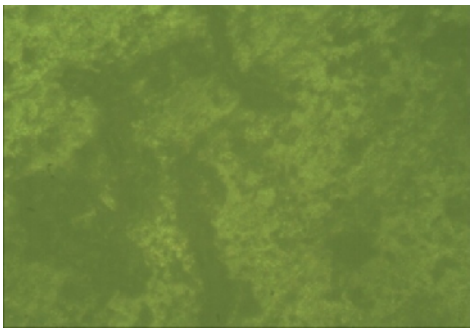

Mild Steel II

Figure 5. Optical micrographs (4X) Aluminium - Control

Visual observation of the low magnification photomicrographs (4X) in **Figure 5** reveals that the surfaces of all the metals in B100 are highly damaged in the experimental systems. Hence to further investigate the surface damage on the test coupons by *Bacillus pumilus* scanning electron micrographs were taken.

4.5.2. Scanning Electron Microscopy

Figures 6 - 10 show the SEM micrographs of the five selected metals aluminium, brass, copper, mild steel I and mild steel II respectively in B100 and CD after exposure to the bacterial system, without removal of corrosion products on the metal surface. It is very clear that the coupons are covered with corrosion products. Aluminium exposed to B100 in the experimental system shows cracks in the corrosion products formed on the metal surface. In brass the metal surfaces exposed to both B100 and CD are covered entirely by the corrosion products. For copper in B100 the surface is covered by the corrosion product in crystalline form which is not obviously seen in CD. Both in mild steel I and mild steel II the products formed are dense and lumpy in B100 as well as in CD.

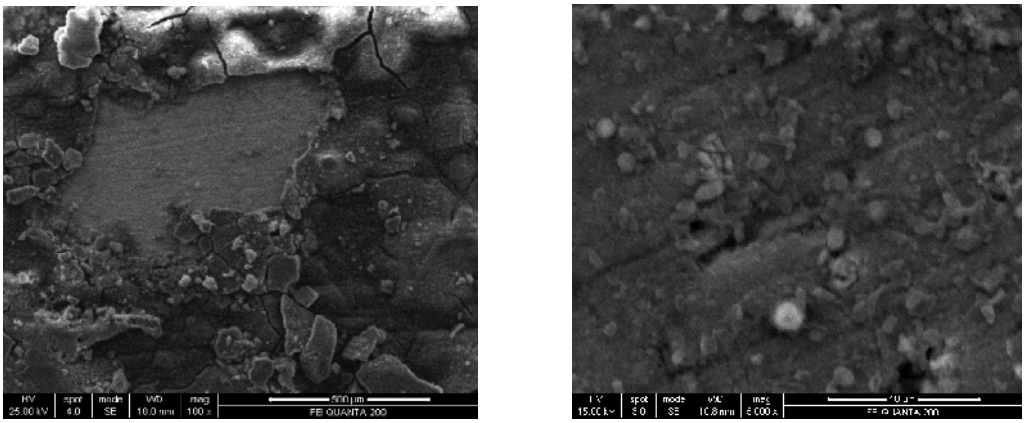

Figure 6. SEM images of aluminium (a) JBD and (b) CD in the experimentalsystem

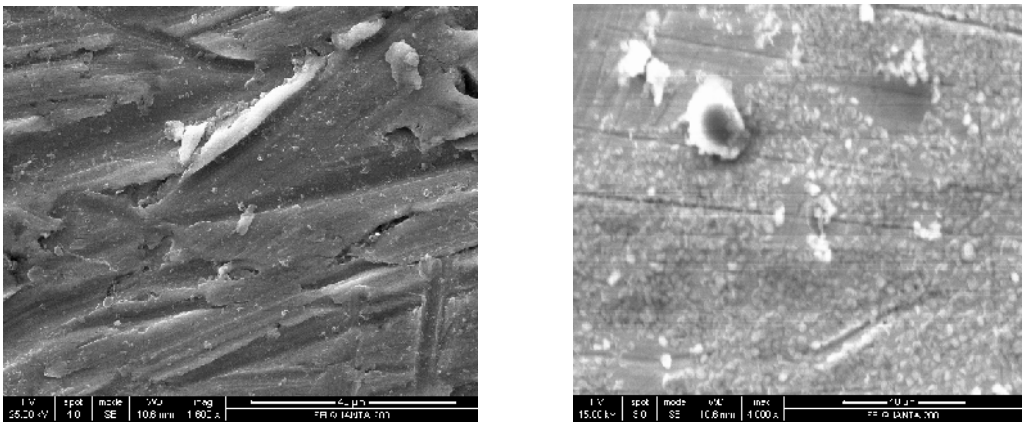

Figure 7. SEM images of brass (a) JBD and (b) CD in the experimental system

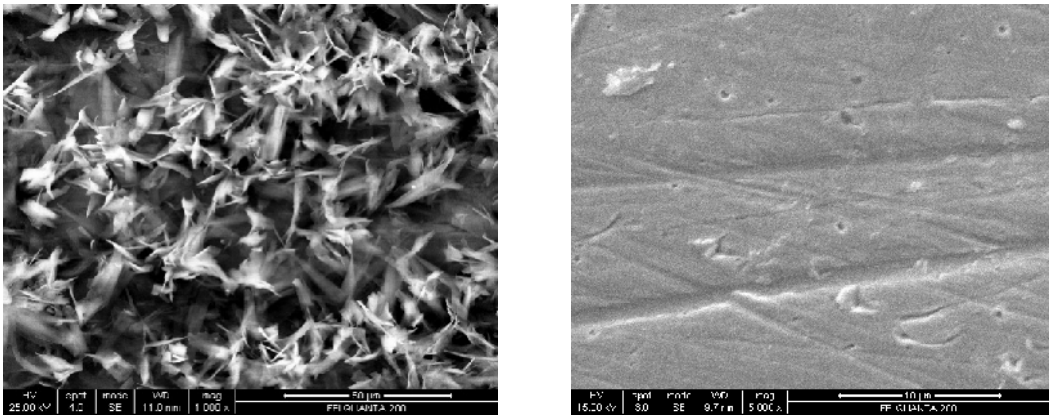

Figure 8. SEM images of copper (a) JBD and (b) CD in the experimental system

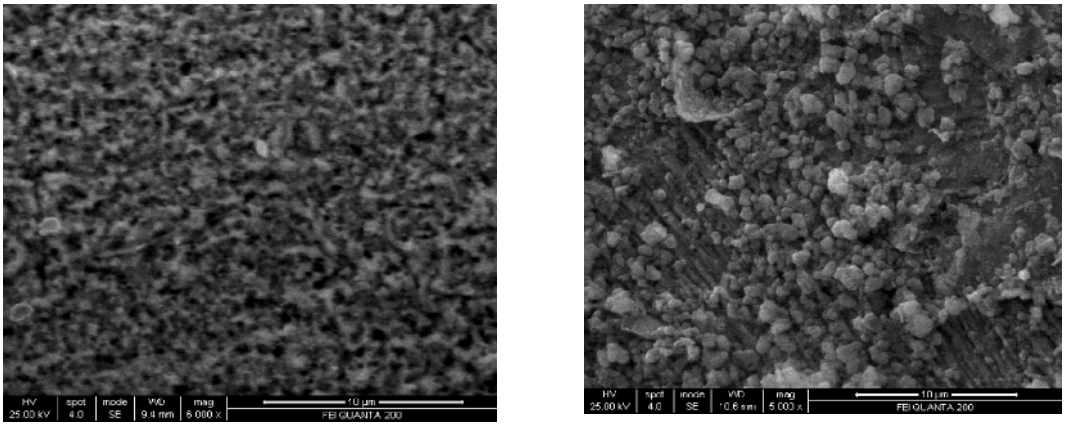

Figure 9. SEM images of mild steel I (a) JBD and (b) CD in the experimental system

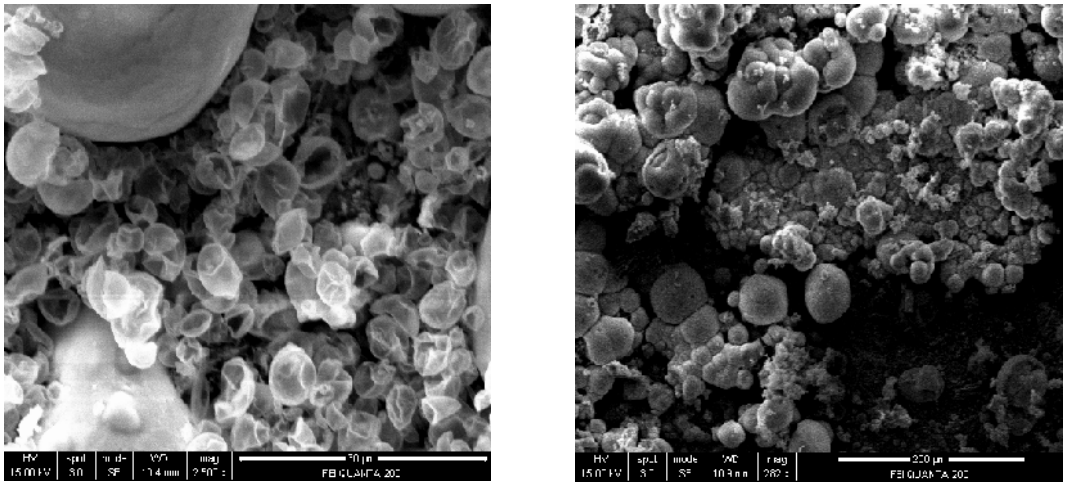

Figure 10. SEM images of mild steel II (a) JBD and (b) CD in the experimental system

4.5.3. Laser profilometry

Laser profilometry is used to determine the surface topography of corroded materials without altering the sample surface through physical contact. Advantages of laser profilometer are

- Automatic in nature – Once the user has defined the scan parameters (area, step size and scan speed) and started the scan, the instrument proceeds with the scan without requiring further input.

- Software packages – Perform a wide range of data operations and analyses

- Surface topography can be imaged in 2 or 3 dimensions.

The surface profile for mild steel II in B100 for the control system is presented in **Figure 11**, and the pit distribution histogram of the mild steel II sample is given in **Figure 12**.

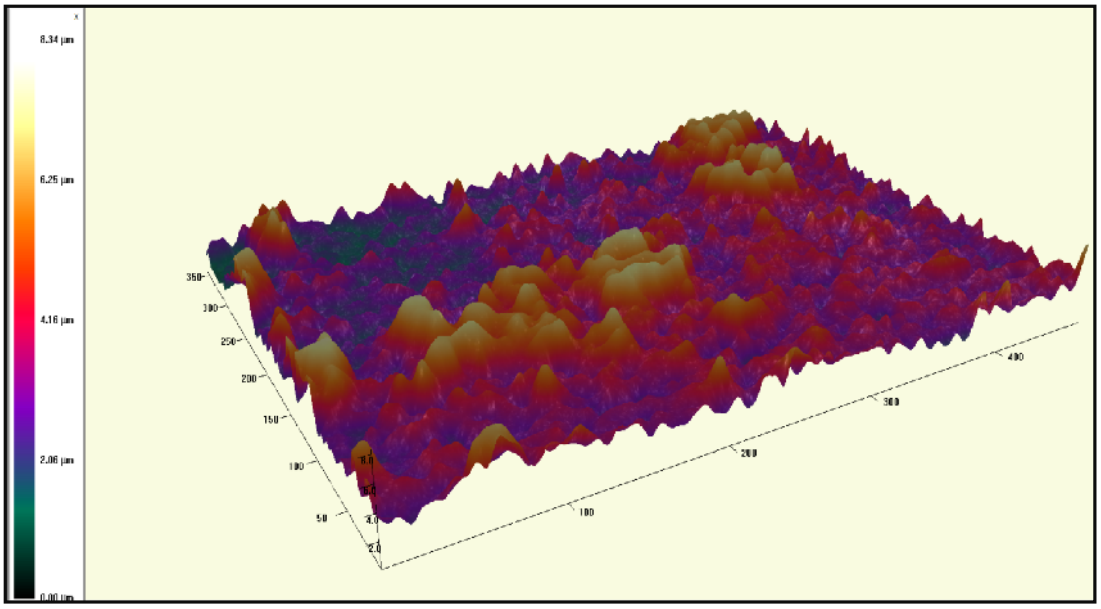

Figure 11. Surface profile (3D image) of mild steel II in control system (B100)

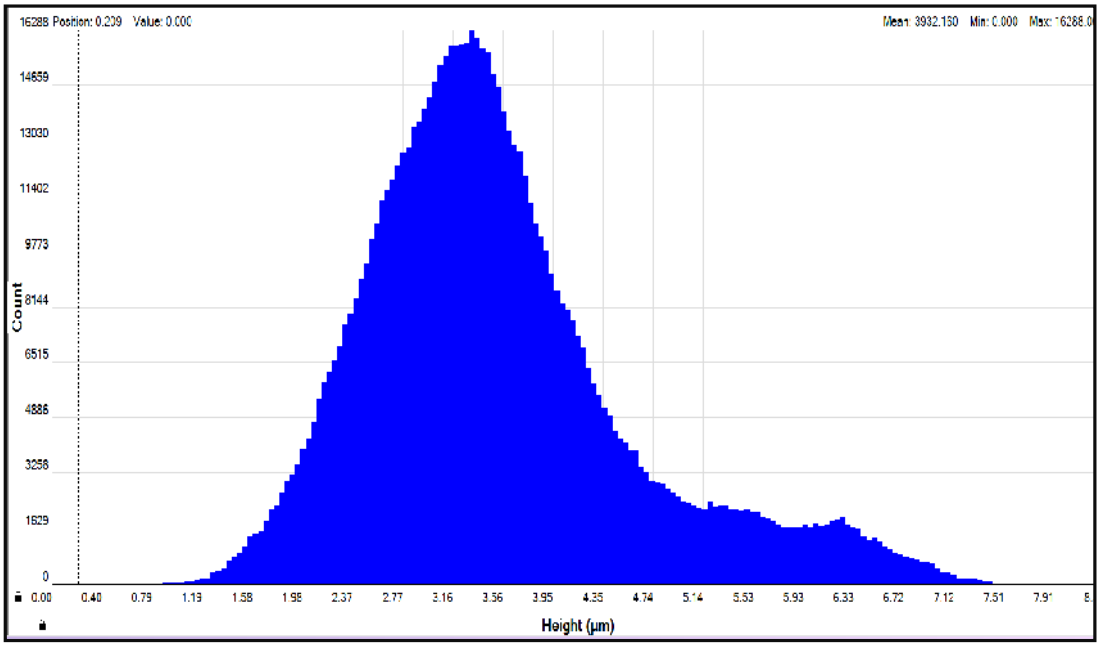

Figure 12 Pit distribution histogram of mild steel II in control system (B100)

The surface profile for mild steel II in B100 for the experimental system is presented in **Figure 13**, and the pit distribution histogram of the mild steel II sample is given in **Figure 14**.

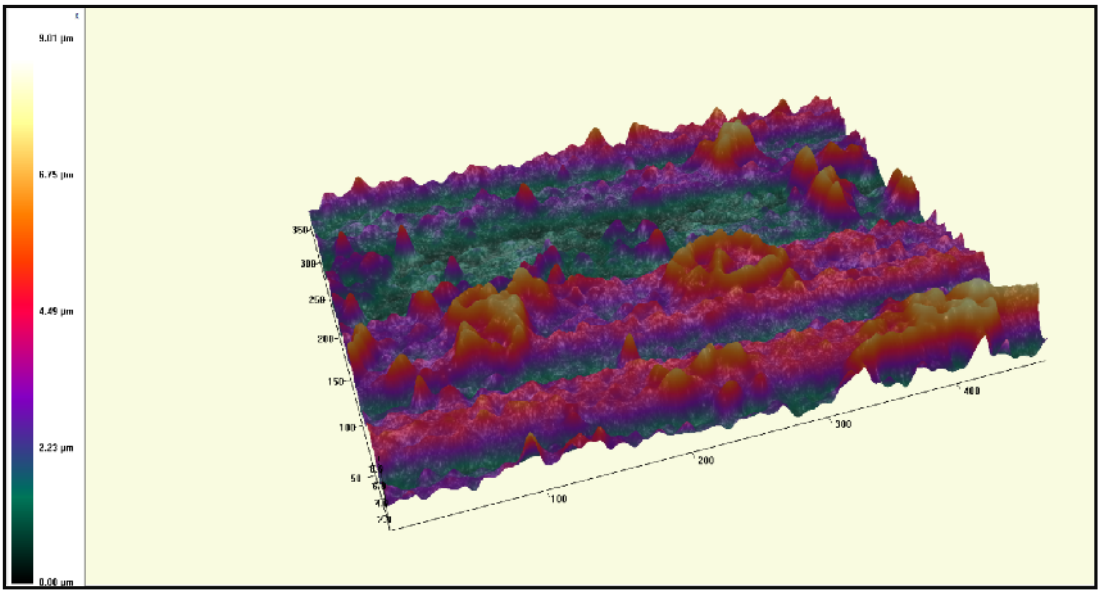

Figure 13. Surface profile (3D image) of mild steel II in experimental system (B100)

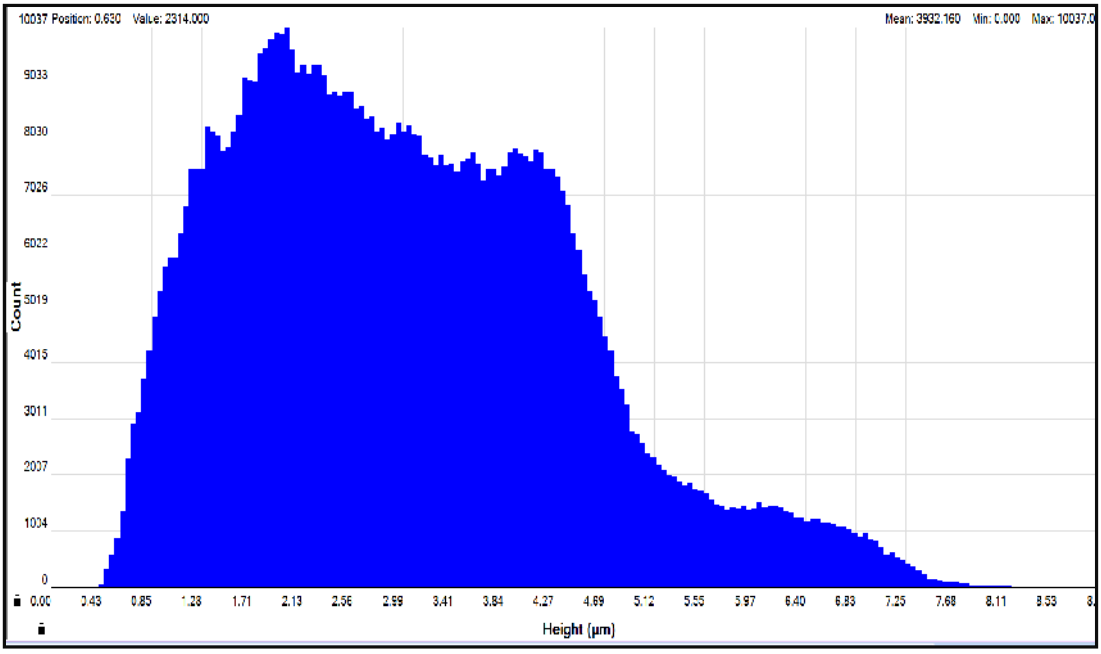

Figure 14. Pit distribution histogram of mild steel II in experimental system (B100)

4.5.3.1. Profile roughness parameters

Corrosion is a surface phenomenon and hence surface roughness which is the measure of texture of a surface is significant in corrosion studies. It is quantified by the vertical deviations of a real surface from its ideal form. If these deviations are large, the surface is rough; if they are small the surface is smooth. The roughness indicates how the real object will interact with the environment and hence often predicts corrosion of metal surfaces. The roughness value is either calculated on a profile (line) or on a surface (area). But the profile roughness parameters are more common. Of the many different roughness parameters used the most common parameters are R_a, R_q and R_t. These parameters are of statistical nature.

R_a is the arithmetic average of the roughness profile.

R_q also known as **R_{rms}** is the root mean square average between the height deviations and the mean line taken over the evaluation length. It describes the finish of optical surfaces.

R_t represents the maximum height – the vertical distance between the highest and lowest point. It describes the overall roughness of the surface.

In the present study the equipment – **Zeta 20 Optical Profiler** determined automatically the profilometric mean roughness parameters R_a, R_q and R_t from the surface profile of the selected metals. Three profilometric scans were taken at different positions on the metal surface, and the mean and the standard deviation were calculated and the results are tabulated in **Table 2** for mild steel II.

Table 2. Roughness parameters for mild steel II

	Control			Experimental		
	R_a (µm)	**R_q (µm)**	**R_t (µm)**	**R_a (µm)**	**R_q (µm)**	**R_t (µm)**
I	0.5197	0.6343	3.524	0.6990	0.8491	3.661
II	0.6591	0.8246	3.987	0.4888	0.6923	4.230
III	0.7769	0.9611	4.309	0.6859	0.8706	4.351
Mean	**0.6519**	**0.8067**	**3.940**	**0.6240**	**0.8040**	**4.081**
SD	**0.1051**	**0.1340**	**0.3219**	**0.0961**	**0.0795**	**0.3009**

From the laser profile data no correlation could be established with mass loss results since mass loss describes the general corrosion while laser profile details localised corrosion.